Exploring the Topological Correlations within Two-Dimensional Foam Structures

A. AbdelKader
College of Humanities and Sciences, Ajman University

E.A. Dawi
College of Humanities and Sciences, Ajman University

A. Haj Ismail
College of Humanities and Sciences, Ajman University

https://doi.org/10.5109/7172259

出版情報：Evergreen. 11 (1), pp.225-233, 2024-03. 九州大学グリーンテクノロジー研究教育センター
バージョン：

Exploring the Topological Correlations within Two-Dimensional Foam Structures

A. AbdelKader[1*], E.A. Dawi[1], A. Haj Ismail[1]
[1]College of Humanities and Sciences, Ajman University, PO Box 346, UAE

*Corresponding author:
E-mail: a.abdelkader@ajman.ac.ae

(Received September 22, 2023: Revised January 15, 2024: Accepted January 19, 2024).

Abstract: This work presents experimental findings on the stability of a 2D foam confined in a hard cell. The foam's lifetime before breakage increases with bubble size, and introducing a defect stabilizes the foam for a few days. Bubble deformations induced by the defects contribute to this stabilization. The study also investigates disorder evolution around defects in a hexagonal lattice. Topological class distributions show an increase in their second moment with some cases showing late-stage decrease. The findings support simulations and offer insights into coarsening and transient phenomena in foams. The research investigates the topological correlations and variations from expected patterns, emphasizing the impact of the particular foam model employed. In addition, the results provide qualitative support for scaling states and suggest generality in defect behavior, and indicate a significant deviation from the expected stability patterns predicted by existing models.

Keywords: Topological correlation; 2D Foam; Cellular patterns; Dry Foam; Polyhedral shapes

1. Introduction

The existence of cellular patterns in nature can be observed in a variety of different places[1)], for example in magnetic domains, crystallized domains in ceramics, biological tissues, and soap froth. Over the past few years, two-dimensional soap froth has been widely investigated for its versatility[2)]. In soap films, gas diffusion is controlled by pressure differences between neighboring cells, which leads to its evolution. A six-sided cell is stable if the internal pressure is the same on all six sides. Foam structure can be described in terms of its degree of 'wetness'. When a liquid containing a large amount of bubbling gas is shaken, foam can be generated if there is a high liquid-to-gas ratio in the liquid. If there is enough liquid content in the mixture, foam appears as spherical bubbles that separate and rise rapidly upward, replacing the heavier liquid. In place of calling the system a foam, it is often referred to as froth or bubbly liquid. Based on the quantity and nature of surface-active components, bubbles in the froth either burst or accumulate into foam once they reach the liquid's surface.

Foam structure can be described with reference to its degree of "wetness". By shaking a liquid containing a large amount of bubbling gas, foam can be generated if the liquid has a high liquid-to-gas ratio. Upon sufficient liquid content, foam appears as spherical bubbles that are separated and rise rapidly upward, replacing the heavier liquid. The system is often referred to as a froth, or a bubbly liquid, rather than a foam. It depends on the quantity and nature of the surface-active components present in the liquid and whether the bubbles in the froth will immediately burst or accumulate to form a foam once they reach the surface of the liquid.

The lack of liquid causes bubbles to depart from their spherical shape, depending on their size distribution. Rather than having spherical bubbles, monodisperse foams containing less than 26% liquid squash the bubbles together[3-5)]. Foams, however, are not mono-disperse, and those containing a liquid content greater than about 5% have bubbles that are roughly cylindrical in shape.bubbles. This system is referred to as a wet foam.

Dry foams have very little liquid, which causes the bubbles to be distorted into approximately polyhedral shapes. Foams containing less than 1% liquid by volume are considered to be this type of foam. As the interfacial area between two adjacent gas bubbles is generally provided by polygonal liquid films of uniform thickness, polyhedral foams are generally made of polygonal liquid films[6,7,8)]. Mechanical constraints determine the regularity of the structure that is produced by these films, even though it is obviously random. An angle of 120º degrees must be maintained whenever three films intersect or meet. Plateau borders are formed by the intersection of these films' borders [9)]. A vertices is formed by the intersecting lines of the Plateau borders; due to mechanical constraints, the only stable vertex is the one that is composed of four borders. A foam structure in a polyhedral form can be distinguished by four junctions connecting groups of four bubbles: first, sets of four bubbles can be perpendicular to each other. Each of these four bubbles shares a vertex, each combination of two bubbles shares a plateau border, and each combination of two bubbles shares a film. According to Durian and Weitz [3)], films are offset by 1200

degrees from each other, while borders are offset by tetrahedral degrees. Furthermore, understanding foam properties is one of the promising methods to overcome gas mobility challenges and use in nanotechnology where a more stable foam can be produced, and has the potential to be used for in the field of solar radiations applications.

The main goal of this research endeavor is to conduct experimental investigations into the progression of disorder within an ideally six-fold coordinated wet foam that encompasses a singular point defect. In addition, the study examines specific topological correlations and patterns that have been previously explored and identified in some simulation models. By looking at experimental and simulation results, we aim to provide a comprehensive understanding of the underlying mechanisms and interactions influencing the foam's structural behavior and disorder development. We briefly discuss spatially separated point defects as well as their interactions. Following are the sections of the paper: Section 2 describes the experimental setup. A discussion and results of the data are presented in section 3. Conclusions and a summary follow in section 4.

2. Experimental Setup

A foam sample can be trapped between two parallel plates to create 2D foam. As a result, perfectly ordered froth appears extremely difficult to achieve. Since bubble rafts are relatively short-lived at the free surface of a soap solution, they are not suitable for studying the evolution of a 2D system. Bubble rafts could be trapped between a glass cover plate and the surface of the solution to avoid this issue. These two-dimensional foam models are generated through the careful structural arrangement and interplay of bubble rafts, contributing distinctive properties that characterize the configuration of the obtained foam. A perfect crystal will, however, exhibit grain boundaries over a wide area even though bubbles naturally form a triangular lattice.

The two-dimensional foam was restricted to a hexagonal shape by our methodology, resulting in a large perfect crystal symmetrical in shape;

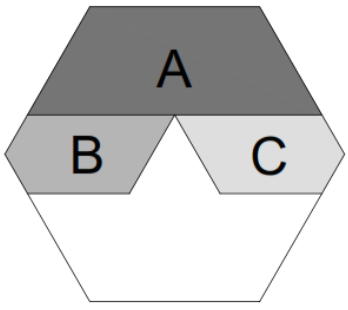

Fig. 1: Schematic illustrating the steps involved in creating a defect. First, a crystalline lattice is fabricated in region A, followed by bubbles being filled in regions B and C, leaving a gap behind. Dislocations are created as bubbles fill in the remaining space.

The two-dimensional array of bubbles on the surface of soap solution has received considerable attention as a model system for condensed matter physics and as an example of two-dimensional foam in recent years. According to previous investigations, a triangular 2D foam of ideally six-fold coordination remained metastable for a short period of time before collapsing. One defect allowed the foam to maintain its stability in this respect despite the introduction of another[11,12].

In view of the meniscus, the ideal 2D foam is metastable as opposed to stable. It is evidenced by the fact that the ideal foam remained stable without capillarity (i.e. without air gaps and meniscus). A bubble exerts force on another based on capillarity and buoyancy. In a study by Nicolson and others, a potential exists between two bubbles. This analysis is not completely appropriate because our bubbles are pushing up against a glass cover and not in direct contact with air. Despite this, we use Nicolson's formulas because they are simple and because an even more precise method would require accurate knowledge of r/r_0 in the initial foam, which we do not possess.

3. Results and Discussion

As perfect as our ideal foam is in its 6-fold coordination, we cannot ignore the fact that the size and separation of these bubbles must also vary. The system seeks to reach equilibrium at $r = r_0$ by small adjustments to the positions of the bubbles resulting in a small readjustment of their positions. This results in some bubbles becoming closer to one another while others become more separated. In order for the system to be more energy efficient, its global energy must be reduced. Over a long period of time, if the accumulation of local stresses within the region is continuous and consistent, it will lead to a progressive weakening in that region, making it more susceptible to various vulnerabilities. When local strain reaches a critical level in this area, cracks appear shortly before the foam breaks.

Stress reaches its peak at about three-quarters of its critical strain (here force/bubble). It is possible that the bubble lattice will rupture if the internal tension exceeds this value. The cohesive strain is defined as the difference between r_0 and r, which corresponds to the maximum force resisting the bubble (i.e. $dV(r)/dr$), which increases monotonically as the bubble diameter increases[13,16].

The cohesive strain between two bubbles was defined by Shi and Argon 8 using the force-displacement law as the ratio of the critical separation distance between the initial equilibrium and the maximum resisted force, to the diameter of the free bubble. We are interested in examining how the size of the bubbles affects the lifetime of an ideal foam. According to the variation in the cohesive strain resulting from the bubble size, the lifetime of the ideal foam increases systematically with the bubble size. When the bubble size increases, the foam requires more strain before it breaks. As a result of the long accumulation time required for the local strain to reach

such a large value, the lifetime of the component will lengthen over time. With the current state of affairs, it is difficult to calculate cohesive strain with a high level of accuracy. The separation between bubbles in the initial foam cannot be precisely determined, but only that it exceeds r_0. In their calculation, Nicolson and Lomer speculated about the possibility of a bubble raft with a free surface, with spherical caps on each bubble; however, in our case, the bubbles are pushed up against the flat cover glass, with the soap films meeting at a 90-degree angle. Consequently, this study uses different boundary conditions than previous studies. The present calculation has been made based on Nicolson's potential as an approximation. The only difference between Lomer's law and an adequate version is the magnitude of the repulsive contribution at r as opposed to above r_0, and it is also more difficult to apply. We calculated r_0 and r to correspond to the inter-bubble forces at different bubble sizes in order to calculate the cohesive strain. In this computation the surface tension of the solution was taken to be 27 mN/m, as discussed above, and Nicolson's tabulations of β and *A* in [17]

$$V_A = (\pi R\sigma\beta^2)RAK_0\left(\frac{r}{a}\right), \qquad (1)$$

where *R* is the radius of the bubble, σ the surface tension of the liquid, β the non-dimensional radius of the circle of contact between the bubble and the fluid surface (b/R), A constant chosen to satisfy the conditions at the inner boundary, and $K_0(r/a)$ the zeroth-order Bessel function where a is the Laplace constant $(\sigma/\rho\ g)^{1/2}$ where ρ is the density of the soap solution.

Based on our lifetime data variations, Figure 2 illustrates a good general agreement regarding cohesive strains against bubble diameter. Nicolson's system differs from ours, which may explain the difference between the theoretical line and the experimental data. Our system is different from Nicolson's system discussed above, which may explain the difference between the theoretical line and the experimental data.

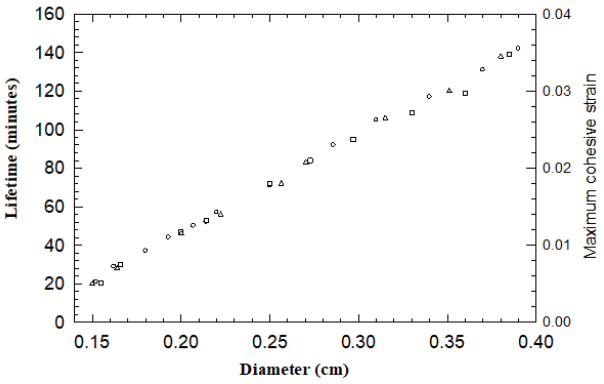

Fig. 2: In hexagonal cells of different sizes, the lifetime of perfect bubble rafts varies as a function of bubble diameter.

According to this definition, the lifespan is the duration during which strain accumulates until it reaches the maximum cohesive strain. Neither the air gap thickness between the soap solution and cover glass nor the thickness of the soap solution seems to have an impact on this. A reduction in the gap results in a more violent breakage of the foam. We conclude, therefore, that the air gap affects the force exerted on the bubbles, while the level of cohesive strain is independent of it. When the meniscus is placed at a long distance, it is necessary that the cover plate be angled at 90 degrees. It is important to note that the inter-bubble potential varies with the meniscus height. A thin air gap with a more curved meniscus must result in a greater force as proportional to dV(r)/dr.

In this section, we will examine the topological correlations in 2D cellular systems. Several correlations, such as the Aboav-Weaire and Lemaitre laws, can be attributed to cellular networks' equilibrium nature. Thus, such correlations are useful to consider in our system. With the use of a certain soap detergent liquid, we were able to run the experiment for a long period of time before the cluster became disordered due to coarsening. This gives us the opportunity to observe the evolution of the cluster as it relates to the defect. Over a long period of time, different experiments were conducted with different topological defects.

As an independent variable, time (t) plays a significant role in simulations [18]. We will observe in our experiments that a number of other factors influence the time evolution of foams containing point defects. In accordance with simulations carried out in [9], the size of the cluster increases over time. Instead of using the length of time as an independent variable, the number of bubbles in the cluster (n_c) may be used.

In Fig. 3, based on simulations, we find that n_c increases with time, as well as n_b for foams containing large bubbles. The latter case shows a close relationship between the two quantities, supporting the conclusion from simulations [19,20] that disorder in the foam propagates outward in response to the growth of the central bubble. Simulations [18] confirm that the boundary is typically only a couple of bubbles wide. It is generally observed that n_c increases smoothly linearly with n_b, but we have found that in some experiments, n_c can actually increase independently of the general trend with n_b, as shown in Fig. 4. Our theory is based on the idea that the cluster was targeted or impacted by other regions, leading to a considerable disorder within those specific areas.

In order to describe the temporal behavior of the present 2D wet foam, a topological transformation can be used [16]. Among the elementary topological processes, there are two primary ones: T_1 (neighbor-switching, when one vertex shrinks to zero, and is replaced by another by its connecting vertex) and T_2 (dispersion of cells in two dimensions). During the early stages of the evolution of certain point defects in 2D foam, distinct sequences of T_1 processes are observed. Cells in the foam exhibit unique patterns as a result of these sequences. The distribution of topological classes of bubbles in the cluster in these

patterns is deterministic, and thus μ'_2 has exact values. The T_2 process tends to occur rarely compared with 2D soap froths. As we will discuss later, this is due to the very small surface area of 3-coordinated bubbles, relative to that of bubbles in the body of the foam.

Our foam is further complicated by the wetness of the current system. The wetness affects the shape of the plateau borders between the bubbles and the triangular shapes of the plateaus lose their triangular shapes as the three-fold borders merge [22]. In scenarios of multiple borders, there can be often a degree of ambiguity regarding the specific adjacency of bubbles. However, it is important to note that even when such potentially complex situations are encountered in practical applications, they are consistently and effectively addressed clearly and straightforwardly.

The neighbors of the bubbles can be defined in two different ways; the first is by defining the touching bubbles and counting the number of bubbles that touch each other which is not significant in our 2D foam with wetness. The other method is to define neighbors based on the nearest bubbles surrounding each bubble, which is known as Voronoi Tessellation. The Voronoi tessellation neighbors are used in our study. It is very difficult to estimate the amount of liquid in our foam, so we compare it with pictures from simulation [21], and we estimate that the liquid fraction (ϕ) in all of our experiments is between 0.97 and 0.93.

The topological and metrical statistics of the cluster are presented based on the different defects. Additionally, there are the number and area of bubbles as well as the second moment (μ_2) of topological class distribution (coordination numbers). A diagram illustrating the topological distribution of bubbles belonging to the cluster can be seen in Fig. 5. There is a clear trend in the graph that the topological distribution function P(n) becomes increasingly large. It appears that n_b increases over time (the cluster becomes more disordered as time passes). Eventually, P(n) became stationary. It is evident from Fig. 6 that the second moment of the topological distribution (μ_2) is linearly increasing with the number of sides of the center bubble (n_b) to a high value where a clear peak can be seen at a certain number of bubbles.

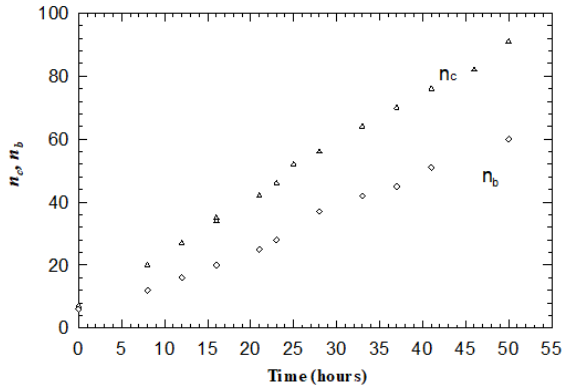

Fig. 3: Variation of n_c and n_b as a function of time.

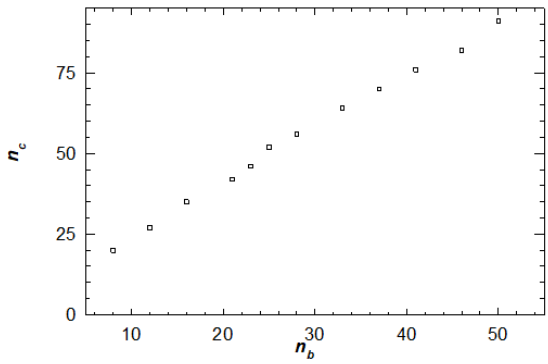

Fig. 4: Comparing bubbles including clusters n_c to bubbles n_b that have topological defects n_b as neighbors.

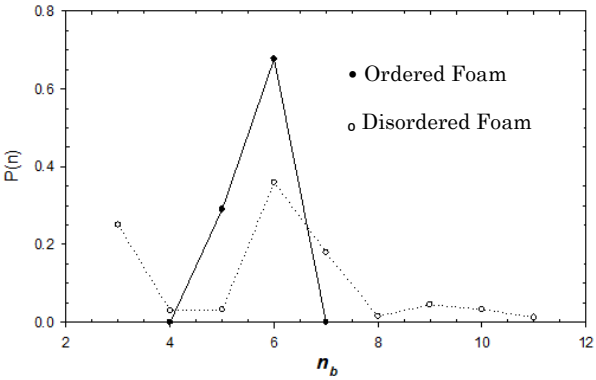

Fig. 5: Topological class distribution P(n) for evolving bubbles containing a topological defect n_b,

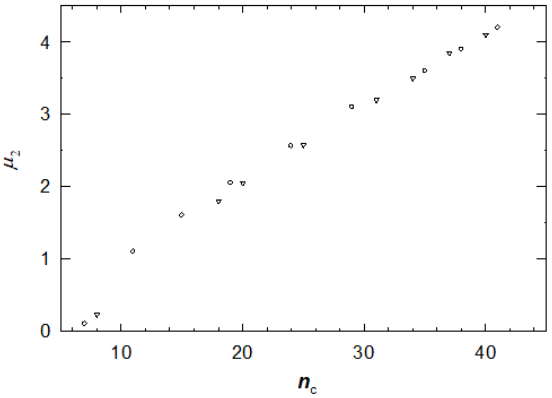

Fig. 6: An analysis of the evolution of the second moment (μ_2) in the cluster with respect to different foams. Data is presented for different point defect.

In our experiments, we achieved diverging values of m_2 which are clearly consistent with those achieved in simulations [19]. In the absence of the large bubble in the center, the second moment of the cluster (the boundary) appears to be saturated at a low value in comparison with μ_2, but in accordance with simulations (Fig. 7).

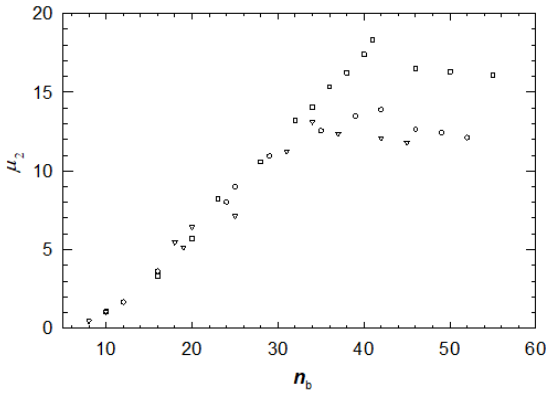

Fig. 7: Different foams evolve at different speeds, and thus the second moment (2) of the cluster changes. Data pointe are for different point defect.

To determine whether our cluster around the defect complies with the Aboav-Weaire law, we now examine the cluster around the defect. As a result, cells that have few sides and many sides have neighboring cells that have few sides and vice versa [1,20].

Previously, Le Caer and Delannay have shown that cells adjacent to an n-sided cell have a mean number of sides of 1 [23], represented by the following equation:

$$m(n) = < n > -a + \frac{<nm(n)> - <n>^2 + <n>a}{n}. \qquad (2)$$

This is the Aboav-Weaire law, which combines two relations, the semi-empirical Aboav's law [22,24]

$$m(n) = A + \frac{B}{n}, \qquad (3)$$

For infinite networks the Aboav-Weaire law has the form usually cited:

$$m(n) = 6 - a + \frac{6a + \mu_2}{n}, \qquad (4)$$

that is due to the fact that Euler's rule implies <n> =6

$$< n > \leq 6 - \frac{12}{N}. \qquad (5)$$

Our data for evolved clusters follows this relation, using n_c as the numeric value for N. However, certain initial states do not follow Euler's rule. Additionally, we found that the data all agreed within 1% of Weaire's sum rule.

It has been pointed out by Weaire that since m(n) is not very dependent upon n, deviations from the law may not be obvious if nm(n) is plotted against n, as is usually done. Accordingly, we plot the data for the various point defects as m(n) against 1/n. It is necessary for the slope and intercept of a linear fit to the data to be consistent in order to claim consistency with the Aboav-Weaire law.

For each type of point defect, the average coordination number of bubbles neighboring n-coordinated bubbles, m(n), is plotted against 1/n in Fig.8. The data are shown in only one set in each case for clarity (usually that of the state at the largest n_c (time), when the cluster should have evolved towards equilibrium). It is important to note that while there are considerable uncertainties regarding the data, there was a consistent trend observed across defects of different types, which suggests that the variations observed are indeed representative of defects of different types. For all types of topological defects (Fig. 8), there is a linear relationship between m(n) and 1/n.

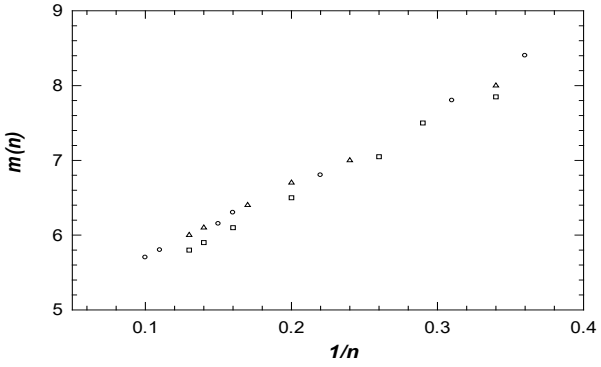

Fig. 8: Variation of the average coordination number of bubbles neighboring n-coordinated bubbles, m(n), against 1/n. Different symbols are for different point defects.

As a general rule, when determining the slope (am) and intercept (ac) of a linear fit, the values of a are mutually consistent, even if they differ according to the case in hand, allowing the Aboav-Weaire law to be applied. Occasionally, our 2D foams do not undergo T_2 processes or cell division, which are not possible in some cases. This can explain the differences between unity and a.

Topological defects, coupled pairs of dislocations, and bubbles of impurities (large and small), however, have consistently nonlinear relationships. A common feature of these types of defects at the end of the experiment was the presence of a population of three-coordinated bubbles. As a consequence, we concluded that the tiny 3-co-ordinated bubbles are responsible for these departures from linearity. As a result, we recalculated m(n) for the clusters, disregarding the 3-coordinated bubbles (concluded to have disappeared as a result of the T_2 process). Thus, the data were computed in the same way as before. Both dislocations and vacancies exhibited linear plots, whereas the other types did not. A closer examination of the distribution of bubbles within the clusters was performed in order to further investigate these differences. In particular, we observed bubble clusters containing large n and large bubbles in the last clusters of dislocations, impurity bubbles, and topological defects (n≥7) in contact with one another. The correlations are not as described by the Aboav-Weaire law. Moreover, due to the positive

association between large bubbles, m(n≥7) is larger than it should be based on the trend for lower n. However, in the case of dislocations and vacancies, evolution does not lead to such associations.

During our experiments, we have taken a randomly selected sample area of foam from within the hexagonal cell when the foam appears much more disordered (large P(6)). A total of 260 bubbles were present in this sample. A linear Aboav-Weaire plot was found for this sample (Fig. 8), where the slope and intercept of a linear fit were consistent with each other. It is evident from the results obtained for some isolated defects that the nonlinear relationships may be due to the short time scales over which our foam evolved from specific initial conditions. There is no evidence that clusters are disordered in spite of dislocations and vacancies. P(6) values confirm that clusters are still ordered in the final stages. It is therefore rather surprising to find linear Aboav-Weaire plots from this perspective. There is no surprise that we observe discordances with the Aboav-Weaire law in some instances since polydisperse cell distributions are expected to depart from linearity in some instances [24]. This large variation in size among the bubbles depicted in Fig. 8 could potentially considered as a contributing factor that accounts for the observed inconsistencies in the figure, mainly when n is set at 3 or surpasses 6.

In another topological correlation involving random 2D cellular structures, μ_2 varies with P(6) in an apparently universal manner. In statistical mechanics, this relation is equivalent to random tessellations of the virial equation of state. In spite of the fact that one might expect virial coefficients to differ from case to case, depending on the form of P(n), this is not the case: data for a very wide range of 2D mosaics can be fitted by a universal curve parameterized by [22,24,25].

$$\mu_2 P(6^2) = 0.15 \pm 0.014. \quad (6)$$

Therefore, all P(n) examined belong to the same universality class [25].

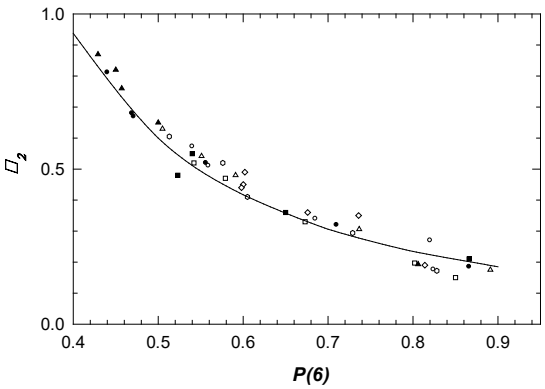

Fig. 9: The second moment (μ_2), with P(6), varies as a function of the foam evolution. Different symbols are for different point defects.

The relationship between μ_2 and P(6) has been examined for all types of defects we have examined. As can be seen in Fig. 9, each cluster represents the evolution of a single defect type. It is reasonable to conclude that the data follow a common trend, but the value of μ_2 for a given P(6) is greater than that for random 2D systems in equilibrium. According to Lemaitre's conceptual framework, our foams appear to follow the 'virial equation' for 2D random systems, but their virial coefficients differ from those previously published [25-28]. This can be attributed to the following reasons: firstly, even at the end of the experiment, our clusters are very orderly. In addition, our foams have an unusually high value of μ_2 due to the presence of 3-coordinated bubbles and the large n bubbles with which they are associated (P(6) preserves the high value of μ_2). Even with all this, it is striking that, although our clusters have their own initial conditions, the data still collapse reasonably well into a common structure. There appears to be little impact on the initial conditions of the clusters. A comparison was also made of μ_2 and P(6) for areas of foam in the initial orderly region (outside the clusters) which became generally disordered. These data were in excellent agreement with the trends shown in Fig. 7.

In the present study, the large values of μ_2 are due to 3-coordinated bubbles, which in the case of froth disappear through T_2 processes even at the late stages of the experiments. In order to investigate this further, we investigated P(n) for the entire foam in the hexagonal cell during its final evolution, when the foam appears to be generally highly disordered. P(n) for this case can be seen to be significantly different from the P(n) for the clusters about the defects. This result is in excellent agreement with Equation 6 and therefore with previous studies [19]. It is not surprising that our clusters obey Lemaitre's law since it applies only to foam in equilibrium.

As part of this section, we present data concerning all types of defects found in the area of the cluster (A_c). Using the image process system which has been mentioned in previous work, the areas of the cluster boundary ($A^{/}$) and of the large central bubble (A_b) are also calculated for impurity bubbles and topological defects. It might be expected that the area of a cluster, Ac, increases linearly with the number of bubbles in the cluster (n_c), as for dislocations.

In the presence of topological defects, the cluster area and the cluster boundary area are plotted against n_c. There is a roughly linear relationship between A_c and $A^{/}$ as n_c increases, as would be expected. To compare with simulations [15,26] we plot A_b against n_b. As we expect A_b to be proportional to n_b^2 in simulations, it is found that A_b is proportional to t^2 while n_b rises roughly linearly with time [19,30,31]. It appears that the neighboring bubble areas decrease with time (increasing n_b): n_b is larger than one would expect for a given Ab due to the departure from the expected n_b dependence. This suggestion is supported by the fact that $A^{/}$ depends on n_c. Thus, the large bubble in the

center determines the total area of the cluster. In the boundary, the average bubble area ($A^{/}$) is normalized to the area of foam ordered at the same age in ordered areas (A_o), falling over time, but fluctuating around a constant value $n_b \geq 20$ (Fig. 10). The average value of $A^{/}/A_o$ is 0.89 ± 0.06 for $n_b \geq 20$ (where μ_2 is constant, indicating that the foam has reached a steady state). This value is quite close to values (0.88 ± 0.08) found in simulations [16], although this value represents the average area of a bubble in the boundary while our value represents the average area per bubble, including Plateau borders which are not insignificant in our wet foam.

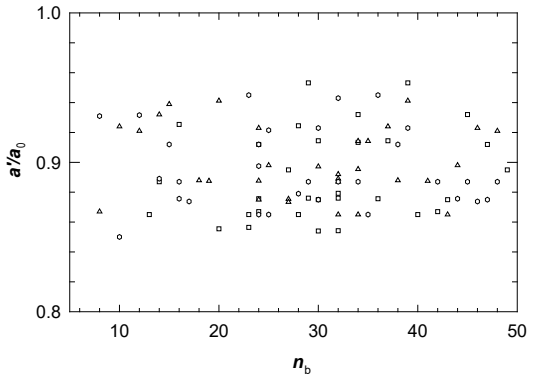

Fig. 10: An evolution of bubble sizes in a foam boundary. It appears that the data points are fluctuating around a stable value. Different symbols are for different point defects.

Geometrical arguments suggest that the number of 6-coordinated cells in the boundary of the cluster n_6 should scale as $\pi\sqrt{n_c}$ (to within a numerical factor of order unity). In the early stages of the experiments, the 6-coordinated cells around the edge of the cluster are all 6-coordinated cells in the cluster. In the late stages of the experiments, a few 6-coordinate cells appear inside the cluster. In order to obtain a reasonable estimate of n_b, we can take n6 as the total number of 6-coordinated cells in the cluster. Our study examines the relationship between n6 and n_c by examining the evolution of a single cluster for each type of defect [32-33,34,35]. According to Fig. 9, n6 grows smoothly with n_c across all sets of data. The variation found, however, deviates from the expected dependence. The continuum treatment inherent in geometrical arguments must fail in low n_c because the area available for internal bubbles is limited. As a result of the irregular outline of large clusters, there is an increased probability of a six-coordinated cell clustering in the cluster (as well as a greater number of bubbles in the six-belt).

4. Summary and Conclusions

Two-dimensional foam stability confined to a rigid cell has been investigated. Foams of this particular type are typically known to have a metastable nature, which implies that they exist mostly in a relatively unstable state that can vary over time. In the case of foams with 6-fold coordination, their metastability leads to breakage around 140 minutes. While these foams are evolving towards their breaking point, there will be a consistent increase in the bubble size throughout their lifetime until the ultimate breakdown occurs. In contrast, introducing a dislocated point or defect stabilizes the foam for a few days during the period of gas disproportion. Bubble deformations caused by elastic stress fields stabilize defects. When the system with a defect tries to achieve equilibrium packing, the energy contribution increases because bubble surface energy and deformation are quadratic.

The present study also investigated the evolution of disorder around single-point defects in an isotropic hexagonal lattice. μ_2 increased with time for all types of defects in the topological class distribution. In some cases, a decrease was also observed at later stages. The decreases are not due to generic factors, but rather to the model foam used. Computer simulations support this conclusion. In foam containing multiple dislocations, they are coarsening which leads to a definite peak in μ_2. Stavans and Glazier's 2D soap froth transient may be explained by the latter observation. A further investigation of the evolution of clusters, the cluster boundary, and the defect has been conducted regarding impurities and topological defects. As a result of our study, we conclude from simulations that the area of disorder that develops around an initial defect (called the boundary) can scale. Various bubbles occur at this boundary; topological classes reach a stationary state with a constant second moment μ_2, and bubble areas remain constant. Our work and simulation results have different wetness values, resulting in various quantitative differences. Furthermore, we have investigated various topological correlations found in random 2D foam models in addition to defects in disordered foam models. Based on the maximum entropy argument, these correlations, like Aboav-Weaire and Lemaitre laws, pertain to statistical equilibrium. Aboav-Weaire plots can emerge in some systems, such as those containing a defect at the outset. We were unable to verify these correlations' generic origins due to limited system statistics. While the Lemaitre law collapses smoothly for all types of defects (m_2 against P(6)), this law shows a distinct variation. It exists because μ_2 is higher than expected for P(6) given the high values of μ_2. Another consequence resulting from the nature of the mode foam was added. We concluded, however, that due to the highest degree of disorder observed, the plot with multiple dislocations may be closer to the universal relationship due to the collapse.

Acknowledgments

This research was funded by Ajman University, Internal Research Grant No: [DGSR Ref. 2023-IRG-HBS-6].

References

1) D. Weaire & N. Rivier (1984) Soap, cells and statistics—random patterns in two dimensions, *Contemporary Physics*, 25:1, 59-99, doi: 10.1080/00107518408210979
2) J Stavans (1993) The evolution of cellular structures, *Rep. Prog. Phys*. 56 733, doi 10.1088/0034-4885/56/6/002
3) D.J. Durian and D.A. Weitz, (1994), Fast, nonevolutionary dynamics in foams, *Current Opinion in Colloid & Interface Science*, 2:6, 615-621 11, 783.
4) D.A Aboav, (1970) The arrangement of grains in a polycrystal, *Metallography*, 3:4, 383-390, doi: 10.1016/0026-0800(70)90038-8.
5) D.A Aboav, (1980) The arrangement of cells in A net, *Metallography*, 13:1, 43-58, doi: 10.1016/0026-0800(80)90021-X.
6) Dunne, Friedrich & Bolton, F. & Weaire, Denis & Hutzler, S.. (2017). Statistics and topological changes in 2D foam from the dry to the wet limit. Philosophical Magazine. 97. 1-14. 10.1080/14786435.2017.1312585.
7) T., Chieco Anthony, P., Sethna James, J., Durian Douglas, Average evolution and size-topology relations for coarsening 2d dry foams, *Frontiers in Soft Matter,* 2, 2022, doi:10.3389/frsfm.2022.941811
8) Yanagisawa, N., Kurita, R. Cross over to collective rearrangements near the dry-wet transition in two-dimensional foams. Sci Rep 13, 4939 (2023). doi: 10.1038/s41598-023-31577-w
9) Ritacco HA. Complexity and self-organized criticality in liquid foams. A short review. Adv Colloid Interface Sci. 2020 Nov;285:102282. doi: 10.1016/j.cis.2020.102282. Epub 2020 Oct 6. PMID: 33059304; PMCID: PMC7537653.
10) M.R. Zakaria, M.F. Omar, M.A. Hazizan Md Akil, M.M. Al Bakri Abdullah. Study of Carbon Nanotubes Stability in Different Types of Solvents for Electrospray Deposition Method. *Evergreen* 7 (4), 538-543, 2020-12, https://doi.org/10.5109/4150473
11) D.F. Smaradhana, D. Ariawan, R. Alnursyah. A Progress on Nanocellulose as Binders for Loose Natural Fibres. *Evergreen* 7(3):436-443 (2020) doi: 10.5109/4068624, https://doi.org/10.5109/4068624
12) A.. Haj Ismail. "Prediction of global solar radiation from sunrise hours using regression functions." *Kuwait Journal of Science* 49 (3) (2022). doi: 10.48129/kjs.15051
13) S. J. Cox, A. M. Kraynik, D. Weaire and S. Hutzler, Ideal wet two-dimensional foams and emulsions with finite contact angle, *Soft Matter*, 14, 5922-5929, 2018, doi: 10.1039/C8SM00739J
14) MA Peshkin & KJ Strandburg & N Rivier, (1991) Entropic predictions for cellular networks. *Phys Rev Lett.* 67:13, 1803-1806. doi: 10.1103/PhysRevLett.67.1803.
15) A. Abd el Kader & J.C. Earnshaw, (1998) Growth of Disorder about Point Defects in Two-Dimensional Foam. *Physical Review E*. 58, 760-770, doi: 10.1103/PhysRevE.58.760
16) L. T. Shi and A. S. Argon, "The potential and force law between different-size bubbles in soap bubble rafts", Philosophical Magazine A, 46:2 255-274 (1982), doi: 10.1080/01418618208239918
17) Nicolson, M. Mathematical proceedings of the Cambridge Philosophical Society, *Math. phys. Sci.*, 45: 288-293 (1949).
18) H.J. Ruskin and Y. Feng, "The evolution of a two-dimensional soap froth with a single defect", J. Phys.: Condens. Matter 7 L553 (1995), doi: 10.1088/0953-8984/7/43/001
19) M. E. Rosa and M. A. Fortes, "Development of bamboo structure in a 2D liquid foam", Europhys. Lett., 41 5 577-582 (1998) doi: 10.1209/epl/i1998-00194-y
20) A.. Haj Ismail, E.A. Dawi, N. Almokdad, A. Abdelkader, and O. Salem. "Estimation and Comparison of the Clearness Index using Mathematical Models - Case study in the United Arab Emirates." *Evergreen* 10 (2) 863-869, (2023). doi: 10.5109/6792841, https://doi.org/10.5109/6792841.
21) A.K.Srivastava, M. Manish, A. Saxena, N.K. Maurya, S.P. Dwivedi. Statistical Optimization by Response Surface Methodology of Process Parameters During the CNC Turning Operation of Hybrid Metal Matrix Composite. *Evergreen* 8(1):51-62 2021 doi: 10.5109/4372260, https://doi.org/10.5109/4372260
22) Dokyum Kim; Yunchang Seol; Yongsam Kim. Numerical study on rheology of two-dimensional dry foam Editor's Pick, *Physics of Fluids*, 33, 052111 (2021) doi: 10.1063/5.0050010
23) D. Weaire, "Some remarks on the arrangement of grains in a polycrystal", Metallography 7(2) 157-160 (1974), doi: 10.1016/0026-0800(74)90004-4.
24) F. Bolton and D. Weaire, "The effects of Plateau borders in the two-dimensional soap froth I. Decoration lemma and diffusion theorem", Philosophical Magazine B, 63:4, 795-809 (1991), doi: 10.1080/13642819108205538
25) G. Le Caer and R. Delannay, "Correlations in topological models of 2D random cellular structures", Journal of Physics A: Mathematical and General, 26 16 3931 (1993), doi: 10.1088/0305-4470/26/16/011
26) M.A.M. Omar Ibrahim, Y. Shigeo. (2018). Experimental and Numerical Studies of a Horizontal Axis Wind Turbine Performance over a Steep 2D Hill. *Evergreen* 5(3):12-21 2018 doi: 10.5109/1957496, https://doi.org/10.5109/1957496
27) N Rivier, (1992) The structure and dynamics of patterns of Benard convection cells, *Journal of Physics: Condensed Matter*, 4:4, doi: 10.1088/0953-8984/4/4/004

28) Anthony T. Chieco, P. Sethna, Douglas J. Durian, Average evolution and size-topology relations for coarsening 2d dry foams, *frontiers*, 22, 2022, doi: 10.3389/frsfm.2022.941811
29) J. J. Chae and M. Tabor, "Dynamics of foams with and without wall rupture", Phys. Rev. E 55, 598, doi: 10.1103/PhysRevE.55.598,
30) M. Fátima Vaz and M. A. Fortes, "Two-dimensional clusters of identical bubbles", J. Phys.: Condens. Matter 13 1395 (2001), doi: 10.1088/0953-8984/13/7/305
31) D. Weaire & M.A. Fortes, "Stress and strain in liquid and solid foams", Advances in Physics, 43:6, 685-738 (1994), doi: 10.1080/00018739400101549
32) C. J. Lambert & D. WEAIRE, "Order and disorder in two-dimensional random networks", Philosophical Magazine B, 47:4, 445-450 ((1983)), doi: 10.1080/1364281.1983.10590681
33) J.B. Chen, J. Gaillardet, J. Bouchez, P. Louvat, and Y.N. Wang, "Anthropophile elements in river sediments: Overview from the Seine River, France", Geochemestry, Geophysics, Geosystems, doi: https://doi.org/10.1002/2014GC005516
34) A. Gervois, J. P Troadec and J. Lemaitre, "Universal properties of Voronoi tessellations of hard discs" Journal of Physics A: Mathematical and General, 25 23 6169 1992, doi: 10.1088/0305-4470/25/23/014
35) A.K. Srivastava, M. Maurya, A. Saxena, N.K. Maurya, S.P. Dwivedi. Numerical and Experimental Study of Flow Behaviours in Porous Structure of Aluminium Metal Foam. Joint Journal of Novel Carbon Resource Sciences & Green Asia Strategy, *Evergreen* 8(3):658-666 2021 doi: 10.5109/4491842, https://doi.org/10.5109/4491842